

Reinvestigating the surface and bulk electronic properties of Cd₃As₂S. Roth,¹ H. Lee,^{1,2} A. Sterzi,³ M. Zacchigna,⁴ A. Politano,⁵ R. Sankar,^{6,7} F. C. Chou,⁷ G. Di Santo,³ L. Petaccia,³ O. V. Yazyev,^{1,2} and A. Crepaldi^{1,*}¹*Institute of Physics, Ecole Polytechnique Fédérale de Lausanne (EPFL), CH-1015 Lausanne, Switzerland*²*National Centre for Computational Design and Discovery of Novel Materials MARVEL, Ecole Polytechnique Fédérale de Lausanne (EPFL), CH-1015 Lausanne, Switzerland*³*Elettra Sincrotrone Trieste, Strada Statale 14 km 163.5, 34149 Trieste, Italy*⁴*C.N.R.–I.O.M., Strada Statale 14, km 163.5, Trieste 34149, Italy*⁵*Fondazione Istituto Italiano di Tecnologia, Graphene Labs, via Morego 30, Genova 16163, Italy*⁶*Institute of Physics, Academia Sinica, Nankang, Taipei 11529, Taiwan*⁷*Center for Condensed Matter Sciences, National Taiwan University, Taipei 10617, Taiwan*

(Received 23 February 2018; published 30 April 2018)

Cd₃As₂ is widely considered among the few materials realizing the three-dimensional (3D) Dirac semimetal phase. Linearly dispersing states, responsible for the ultrahigh charge mobility, have been reported by several angle-resolved photoelectron spectroscopy (ARPES) investigations. However, in spite of the general agreement between these studies, some details are at odds. From scanning tunneling microscopy and optical experiments under magnetic field, a puzzling scenario emerges in which multiple states show linear dispersion at different energy scales. Here, we solve this apparent controversy by reinvestigating the electronic properties of the (112) surface of Cd₃As₂ by combining ARPES and theoretical calculations. We disentangle the presence of massive and massless metallic bulk and surface states, characterized by different symmetries. Our systematic experimental and theoretical study clarifies the complex band dispersion of Cd₃As₂ by extending the simplistic 3D Dirac semimetal model to account for multiple bulk and surface states crossing the Fermi level, and thus contributing to the unique material transport properties.

DOI: [10.1103/PhysRevB.97.165439](https://doi.org/10.1103/PhysRevB.97.165439)**I. INTRODUCTION**

Since their theoretical prediction [1], three-dimensional Dirac semimetals (DSMs) are fascinating the condensed-matter community in consideration of their high potential for applications. DSMs represent the three-dimensional (3D) extension of graphene, with linearly dispersing bulk states. The fourfold degenerate bulk Dirac point can result from an accidental gap closure, as in the case of BiTl(S_{1-δ}Se_δ)₂ [2] or ZrTe₅ [3,4], or it can be topologically protected by symmetries, such as invariance of the system under rotation [5]. DSMs can display exotic surface states evolving into surface Fermi arcs under the breaking of spin degeneracy, which splits the single Dirac point into two chiral Weyl points [6].

Among the DSMs, Cd₃As₂ is the most investigated system [7–18]. Its electronic properties have been investigated by several angle-resolved photoelectron spectroscopy (ARPES) studies [8–12]. Bulk states exhibit linear dispersion over a wide energy range, up to several eV [8]. The occurrence of 3D Dirac fermions has been connected to the material's ultrahigh mobility and giant magnetoresistance [13], which might find application in devices such as ultrafast broadband photodetectors [14,15].

Despite the general agreement between the ARPES experiments, details of the band structure remain still unex-

plained. First of all, the existence of a 3D Dirac point is protected by the C₄ rotational symmetry only along the Γ Z direction, corresponding to the (001) surface termination [7] not accessible to ARPES, as the natural cleavage plane is the (112) termination [9,16]. Nevertheless, ARPES studies have reported the existence of a sharp *n*-doped Dirac cone [9,10], whose dimensionality shows no clear 3D periodicity [9] and it was proposed to acquire two-dimensional (2D) character upon alkali-metal evaporation [12]. The scenario becomes even more puzzling if the gaze is turned to other experimental techniques. The energy scale of the dispersion of the symmetry-protected Dirac particles is strongly rescaled. Scanning tunneling spectroscopy under magnetic field reveals Landau levels which are compatible with a shallow band inversion, of the order of 20 meV [17]. Finally, a recent full optical study under magnetic field has proposed that the band structure of Cd₃As₂ is better described in terms of massless Bodnar-Kane electrons, linearly dispersing over a large energy scale [18].

In this paper we have reinvestigated the band structure of (112)-terminated Cd₃As₂, by means of a joint experimental and theoretical study aimed at reconciling apparent controversies in previous ARPES studies [8–12]. In particular, we focus our attention on the number and dimensionality of the low-energy electronic states. By carrying out a detailed polarization-dependent ARPES study, we disentangle the existence of multiple states crossing the Fermi level, E_F . Such states exhibit different photon energy dependence and a clear signature of the simultaneous presence of both surface and bulk states.

*alberto.crepaldi@epfl.ch

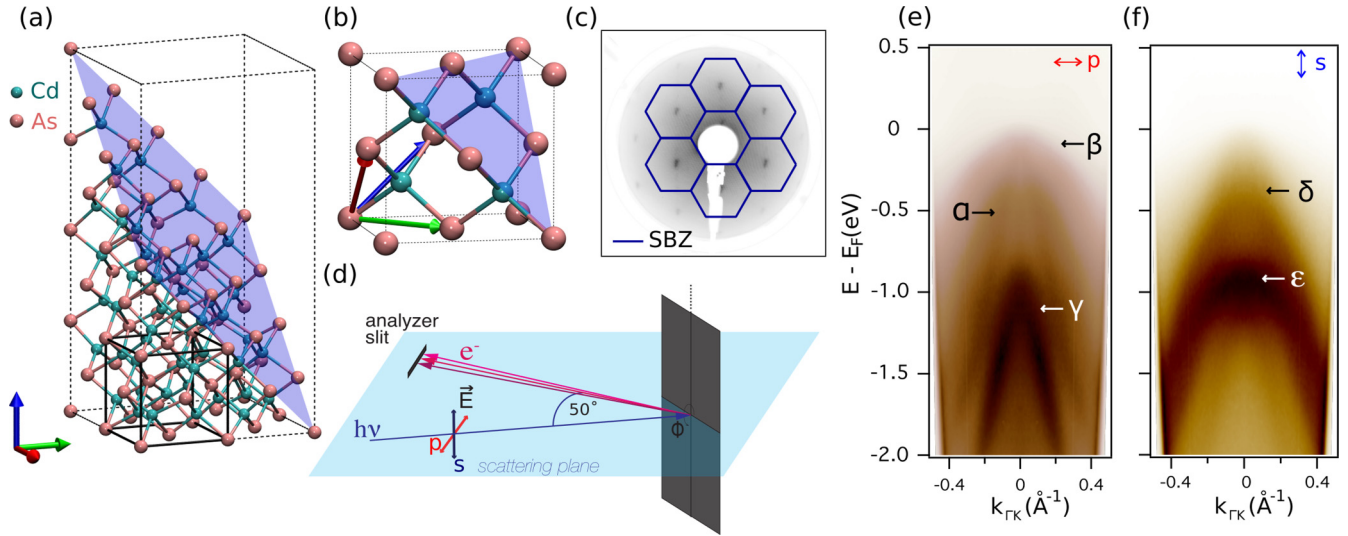


FIG. 1. (a) Crystal structure of Cd_3As_2 characterized by space group $I4_1cd$ and lattice parameters $a = 12.65 \text{ \AA}$ and $c = 25.44 \text{ \AA}$ [19]. (b) Reduced zinc-blende unit cell used in our model Hamiltonian. (c) Low-energy electron diffraction (LEED) image of a freshly cleaved Cd_3As_2 sample. The first-order diffraction spots are arranged in the pseudo-hexagonal symmetry characteristic of the (112) natural cleavage plane [16]. Blue lines indicate the surface Brillouin zone. (d) Experimental geometry of the BaDElPh beamline. The analyzer entrance slit lies in the scattering plane and the measurements have been carried out at normal emission. The p and s light polarization, indicated with red and blue arrows, are selectively probing only the even and odd states with respect to the crystal symmetry plane. (e), (f) ARPES image of the Cd_3As_2 band dispersion along the $\bar{\Gamma}\bar{K}$ surface high-symmetry direction, measured with 20 eV photon energy and p and s polarization, respectively. States with different parities are probed, and they are labeled with greek letters.

Specifically, our findings are consistent with the existence of a 3D state highly dispersing up to several eV below E_F , similar to what was observed in Ref. [8]. Moreover, we reveal a sharp Dirac cone which closely resembles the one previously reported by other ARPES studies [9,10], and proposed to bear a signature of the DSM phase. However, on the basis of our photon-energy-dependent study we conclude that this is related to a surface Dirac particle. Our theoretical calculations support the existence of several bands, characterized by different symmetries and by both bulk and surface character. Overall, our observations indicate that Cd_3As_2 cannot be simply taken as a prototypical DSM, but a more realistic model has to be adopted to account for the presence of multiple states crossing E_F and contributing to the charge transport properties while having different effective masses.

II. EXPERIMENTAL AND THEORETICAL METHODS

High-quality Cd_3As_2 single crystals were grown by self-selecting vapor growth, as described in detail in Ref. [19]. Cd_3As_2 can adopt two possible body-centered tetragonal structures, of defect antiferrotype [16], with either noncentrosymmetric $I4_1cd$ space group [20] or with centrosymmetric space group $I4_1/acd$, depending on the growth conditions [19]. The crystals that are the subject of our study belong to the noncentrosymmetric $I4_1cd$ space group, as determined by detailed x-ray diffraction studies [19].

Figure 1(a) shows the crystal structure, with lattice parameters $a = 12.65 \text{ \AA}$ and $c = 25.44 \text{ \AA}$ [19]. The unit cell contains 32 formula units, and the resulting large number of atoms per cell has hampered a direct calculation of the electronic band structure, so far. For circumventing this problem, a simplified

model Hamiltonian has been developed [8,11]. The model is based on a primitive zinc-blende cell formed by As ions in an fcc lattice and Cd ions occupying one half of the tetrahedral holes, as schematized in Fig. 1(b).

Our first-principles model Hamiltonian is constructed using as a basis the maximally localized Wannier functions (WFs) [21] obtained from density-functional theory (DFT) [22] calculations. WFs are generated using the WANNIER90 code [23] and the inputs to WANNIER90, overlap and projection matrices, are obtained from DFT calculations within the generalized gradient approximation [24] for the exchange-correlation energy as implemented in QUANTUM ESPRESSO [25]. The bulk and surface band dispersions are obtained from the \mathbf{k} -resolved local density of states which are calculated from the surface Green's function of the semi-infinite system using the iterative algorithm [26]. The on-site energies of s -like WFs at Cd are chosen so that the resulting bulk- and surface-state dispersions are able to capture the main features in the ARPES data as similarly done in Refs. [8,11]. Considering the parity of polarized light with respect to the mirror plane in the ARPES setup, s -like WFs at Cd and p_y (p_z)-like WFs at As are used for simulating the ARPES data measured with p -polarized light and p_x -like WFs at As for that with s -polarized light.

The Cd_3As_2 crystals are cleaved in ultrahigh vacuum (UHV) by post-method. The natural cleavage plane occurs on the (112) surface, indicated by a light-blue plane in Fig. 1(a), and leaves large terraces ideal for ARPES experiments. Figure 1(c) shows a low-energy electron diffraction (LEED) image of a freshly cleaved surface. The first-order diffraction spots are arranged in a pseudo-hexagonal symmetry, as expected for the (112) termination [8,16,19], and the corresponding surface projected Brillouin zone (SBZ) is outlined

in blue. The ARPES experiments have been carried out at the BaDElPh beamline at the Elettra synchrotron, in the energy range 20–34 eV [27]. The sample temperature was set to 80 K, and the analyzer energy and angular resolution were 15 meV and 0.2° , respectively. A schematic drawing of the experimental geometry is depicted in Fig. 1(d). The analyzer entrance slit lies in the scattering plane defined by the incoming photons and the photoemitted electrons. In contrast to previous ARPES studies, our geometry can fully select the parity of the investigated bands. In particular, p - (s -) polarized photons probe purely even (odd) states with respect to the material symmetry plane. In principle, circularly polarized light would have granted simultaneous access to all the states, although making their identification more difficult. We notice that the Cd_3As_2 crystals exhibit a high surface reactivity, even in a pressure $< 5 \times 10^{-11}$ mbar, with a fast process of p -type doping which takes place in the first minutes after cleave, which we will discuss later. In principle, this energy evolution of the band structure as a function of time can affect a proper investigation of the material's band dispersion. In order to account for this problem, all the data shown here have been acquired in stationary conditions, when no further evolution of the chemical potential in the band structure was detected.

III. RESULTS

The comparison between ARPES data acquired with different light polarization helps in clarifying the material band dispersion. Figures 1(e) and 1(f) show the ARPES acquired with 20 eV photon energy along the $\bar{\Gamma}\bar{K}$ high-symmetry direction of the SBZ, with p - and s -polarized light, respectively. We clearly distinguish different bands which we labeled with greek letters. For p -polarized light, in Fig. 1(e), we resolve two bands α and β crossing the Fermi level, while a third one, γ , reaches its maximum dispersion ~ 1 eV below E_F . The sharp and linearly dispersing α band immediately strikes our attention, in contrast to the rather broad parabolic spectral distribution of the other bands. This band closely resembles the one reported by previous ARPES studies [9, 10], and its nature will be discussed in detail in the following. After switching to s -polarized light, two different bands become visible, which we label δ and ϵ , and the former is found to cross E_F .

The remarkably broad dispersion of the δ band suggests its possible bulk origin, which we have further investigated by carrying out a photon-energy-dependent study. Figures 2(a)–2(c) show the band dispersion at E_F for selected photon energies (24.0, 27.5, and 31.0 eV, respectively) along the $\bar{\Gamma}\bar{K}$ direction. We estimate the corresponding k_z wave vectors by using the inner potential value $V_0 = 10.6$ eV as proposed by Liu *et al.* [8]. In fact, our investigated photon energy range is not sufficient to fully cover the whole 3D BZ; however, it grants access to the momentum region close to the bulk Γ point, where the bulk Dirac point is expected to be located, according to a previous study [8]. The δ band clearly exhibits a large 3D dispersion; it approaches E_F when the photon energy is varied between 20 and 24 eV, and it disperses away from E_F for larger photon energies up to 34 eV.

The evolution of the spectral weight at the Fermi level is more clearly illustrated by the momentum distribution curves

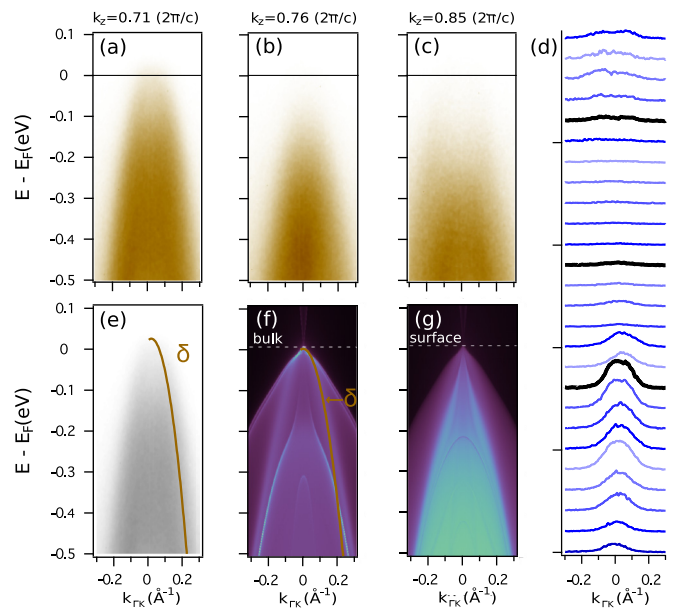


FIG. 2. (a)–(c) Band dispersion of Cd_3As_2 along the $\bar{\Gamma}\bar{K}$ high-symmetry direction of the SBZ, measured with s -polarized light for 24, 27.5, and 31 eV photon energy, whose corresponding k_z values are indicated. (d) Stack of MDCs in the measured photon energy range, 20–34 eV with 0.5 eV step. Each MDC is integrated 15 meV across E_F , and they are displayed with a vertical offset. The photon energy increases from the bottom to the top, and black lines correspond to the data displayed in (a)–(c). (e) ARPES image of the data taken at 24 eV displayed along with a guideline (brown) of the δ band dispersion. (f) and (g) Calculated band dispersion for the zinc-blende model Hamiltonian. The calculations show only states with odd parity, compatible with the experimental geometry, for (f) the bulk and (g) at the Cd-terminated (112) surface.

(MDCs) of Fig. 2(d). They are integrated over a 15 meV energy window centered at E_F from the ARPES images acquired in the photon energy range 20–34 eV, with 0.5 eV energy step. For the sake of visibility, the MDCs are displayed with a vertical offset and the photon energy increases from the bottom to top. Black lines correspond to the photon energies of panels (a)–(c). The intensity at E_F is maximum for the photon energies between 23 and 24 eV. Figure 2(e) shows the ARPES data corresponding to a photon energy of 24 eV, along with a brown guideline tracing the band dispersion. The band dispersion is well accounted by a parabolic dispersion, with effective mass $m^* \sim 0.23m_e \pm 0.02m_e$. From a linear fit, we estimate the band velocity at the Fermi level to be $v \sim (5.2 \pm 1) \times 10^5$ m/s, a value which is slightly smaller than what is reported from transport measurement [13], but in agreement with previous ARPES studies [8, 9].

Figures 2(f) and 2(g) illustrate the results of our model calculations, for the simplified zinc-blende structure. Here we focus on the states with odd parity, in the bulk and at the Cd-terminated (112) surface. We have indicated with an arrow in Fig. 2(f) the dispersion of the δ band. We immediately notice that states with odd parity mainly contribute to the valence band and only very weak intensity can be found above E_F , thus indicating that the upper part of the 3D Dirac cone would escape detection with s -polarized photons.

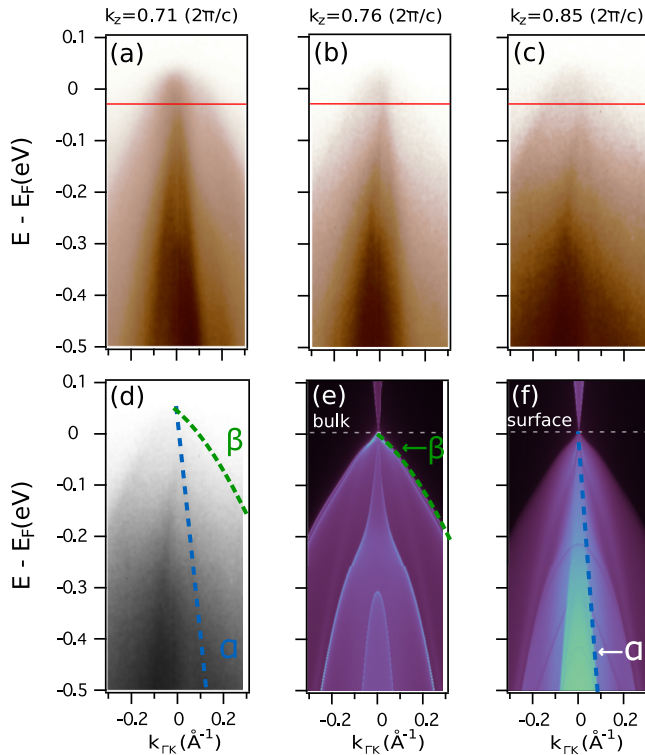


FIG. 3. (a)–(c) Band dispersion of Cd_3As_2 along the $\overline{\Gamma K}$ high-symmetry direction, measured with p -polarized light for 24, 27.5, and 31 eV photon energy. (d) ARPES image of the data acquired at 31 eV along with guidelines for the α (blue) and β (green) bands. (e) and (f) calculated band dispersion for the zinc-blende model Hamiltonian. The calculations show only states with even parity, in (e) the bulk and (f) at the (112) surface.

In the following, we will discuss data acquired with p -polarized photons, assessing the states with even parity. In particular, we turn our attention to the linearly dispersing α state observed in Fig. 1(e). A similar sharp state has been reported by previous ARPES studies of Cd_3As_2 [9,10]. However, the dimensionality of this linearly dispersing band is still unclear. In fact, the previous studies only reported the presence/absence of α at different photon energies [9,10]. The presence of a Dirac point along the $\overline{\Gamma Z}$ high-symmetry direction was supported by the lack of a well-defined k_z periodicity [9]. To correctly address the character of this state, we have investigated its photon energy dependence. Figure 3 shows the band dispersion along $\overline{\Gamma K}$ for selected photon energies (24.0, 27.5, and 31.0 eV). The α state linearly disperses across E_F over the investigated photon energy range of 20–34 eV. The band disperses linearly with $v \sim (6.5 \pm 1) \times 10^5$ m/s and it forms a Dirac point, located $\sim 0.03 \pm 0.01$ eV below E_F , indicated with red lines in Figs. 3(a)–3(c). Our data do not reveal any signature of k_z dispersion in the α state, which thus is ascribed to a 2D surface Dirac fermion band.

The observation of a linearly dispersing surface state is supported by our theoretical calculations, shown in Figs. 3(e) and 3(f) for the even-parity states in the bulk and at the (112) surface. The dispersion of α is well reproduced by our model Hamiltonian for the surface termination, Fig. 3(f).

The existence of a surface Dirac particle was proposed also by Yi and co-workers [11], in agreement with theoretical predictions [7]. Thanks to our capability to distinguish states with different parities, our data further extends previous results by disentangling the dispersion of the surface state α from that of the bulk state δ . Furthermore, in p polarization we resolve a second state dispersing across E_F , β . Figure 3(d) reports the data acquired at a photon energy of 31.0 eV, with blue and green lines indicating the dispersion of α and β , respectively. The latter exhibits also very weak k_z dispersion [see Figs. 3(a)–3(c)]. The theoretical calculations shown in Fig. 3(e) indicate that β is a bulk state. The bulk nature of β may also explain its spectral broadening. As a matter of fact, while α is sharp and well defined over the investigated photon energy range, β appears blurred, similarly to the bulk δ state. We propose that, in comparison to δ , the weaker k_z dispersion of β reflects its larger effective mass. This is supported by the direct comparison between the in-plane effective masses. Along $\overline{\Gamma K}$, β is well approximated by a parabolic dispersion with $m^* \sim 1.58m_e \pm 0.05m_e$, shown by the green line in Fig. 3(d). This value is almost seven times larger than the corresponding one estimated for δ . Hence, we argue that β might play the role of the flat heavy-hole band expected in the Bodnar-Kane model, which was proposed by optical experiments under magnetic field to provide a better description for the low-energy band structure of Cd_3As_2 [18].

Finally, experimentally we notice that β reaches its maximum $\sim 0.04 \pm 0.01$ eV above E_F . Also the δ band is found to disperse above E_F , while the Dirac point of α is located below E_F . These fine details of the material band structure cannot be fully captured by the model Hamiltonian, but they indicate that the charge neutrality points for the surface and bulk states are not degenerate. Interestingly, we observe the ambipolar character of the charge carrier: electrons in the surface state α and holes in the bulk states β and δ . However, this finding can be proven only in the surface region, due to the ARPES surface sensitivity.

A precise estimation of the material doping from ARPES measurements is hampered by the evolution of the Fermi level within the band structure, which was unnoticed in the previous ARPES studies [8–12]. Figure 4 summarizes this effect, and the capability to tune the surface doping via deposition of alkali-metal atoms. The data corresponds to the $\overline{\Gamma K}$ direction measured with p -polarized photons at 25.0 eV. Figure 4(a) shows that the surface Dirac cone α is strongly n -doped in the freshly cleaved surface, and the Dirac point is located 200 meV below E_F , in agreement with other ARPES studies [9,10,12]. Figures 4(b) and 4(c) display the evolution of the chemical potential after 30 min and 2 h, respectively.

Upon K deposition, the bands are shifted back at larger binding energy, Fig. 4(d). However, this surface doping is not stable and a tendency to p -type doping persists in time, as reported in Figs. 4(e) and 4(f). The same effect is visible also after a second K deposition [see Figs. 4(g)–4(i)]. The evolution of the chemical potential has been investigated only with horizontal polarization, and we did not resolve different behaviors for the bulk and surface states. However, Figs. 4(a)–4(c) show that the contrast between the α and β states evolves with time and the bulk β band is more visible at the aged surface, Fig. 4(c). The evolution of the

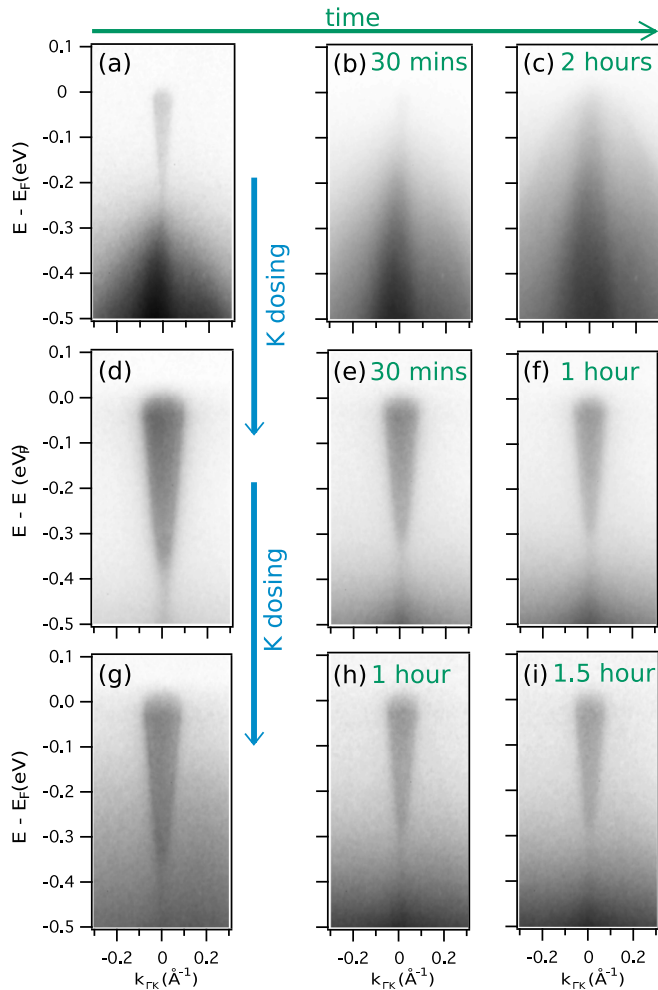


FIG. 4. (a)–(c) Evolution of the chemical potential of Cd_3As_2 along the $\bar{\Gamma}\bar{K}$ high-symmetry direction, measured with p -polarized light at 25 eV for (a) the freshly cleaved surface, (b) after 30 min, and (c) after 2 h. (d)–(f) ARPES images after the first K deposition; the bands are initially shifted toward larger binding energy (d) but with time the system experiences a tendency to p -type doping. (g)–(i) Similar ARPES images after a second K deposition.

band structure upon alkali-metal deposition onto Cd_3As_2 was already reported in a previous ARPES study [12]. However, we

stress that our results of Fig. 3 clearly show that the linearly dispersing α is a surface state, and its surface character is not a consequence of the K deposition, in contrast with previous conclusions [12].

IV. CONCLUSIONS

In summary, herein we have reinvestigated the band structure of Cd_3As_2 by combining theoretical calculations and polarization- and photon-energy-dependent ARPES measurements of the (112) surface termination. By varying the light polarization we selectively probe states with odd and even parities, thus resolving the dispersion of three different states across the Fermi level. The states exhibit different dispersion as a function of the incoming photon energy. We observe a sharp n -doped Dirac cone with no k_z dispersion, which we interpret as a 2D surface Dirac fermion band in agreement with a similar finding [11]. Furthermore, we reveal the dispersion of two bulk states, characterized by different parities and effective masses. In addition, we provide evidence for the evolution of the chemical potential within the band structure, as a function of time.

We believe that our results help in clarifying the band dispersion of Cd_3As_2 , a compound widely considered among the few materials realizing the 3D DSM. However, our study shows that the description in terms of 3D DSM is simplistic, and a more realistic model has to be adopted to account for the presence of multiple states crossing E_F with different effective masses and all contributing to the charge transport properties.

ACKNOWLEDGMENTS

We acknowledge clarifying discussions with A. Akrap. We acknowledge financial support by the Swiss National Science Foundation. This work was supported in part by the Italian Ministry of University and Research under Grants No. FIRBRBAP045JF2 and No. FIRB-RBAP06AWK3 and by the European Community Research Infrastructure Action under the FP6 “Structuring the European Research Area” Program through the Integrated Infrastructure Initiative “Integrating Activity on Synchrotron and Free Electron Laser Science,” Contract No. RII3-CT-2004-506008. H.L. and O.V.Y. acknowledge support by the NCCR Marvel and the ERC Starting Grant “TopoMat” (Grant No. 306504). First-principles calculations have been performed at the Swiss National Supercomputing Centre (CSCS) under Project No. s675.

- [1] S. M. Young, S. Zaheer, J. C. Y. Teo, C. L. Kane, E. J. Mele, and A. M. Rappe, *Phys. Rev. Lett.* **108**, 140405 (2012).
- [2] S.-Y. Xu, M. Neupane, I. Belopolski, C. Liu, N. Alidoust, G. Bian, S. Jia, G. Landolt, B. Slomski, J. H. Dil *et al.*, *Nat. Commun.* **6**, 6870 (2015).
- [3] H. Weng, X. Dai, and Z. Fang, *Phys. Rev. X* **4**, 011002 (2014).
- [4] G. Manzonei, L. Gragnaniello, G. Autès, T. Kuhn, A. Sterzi, F. Cilento, M. Zacchigna, V. Enenkel, I. Vobornik, L. Barba *et al.*, *Phys. Rev. Lett.* **117**, 237601 (2016).
- [5] B.-J. Yang and N. Nagaosa, *Nat. Commun.* **5**, 4898 (2014).
- [6] X. Wan, A. M. Turner, A. Vishwanath, and S. Y. Savrasov, *Phys. Rev. B* **83**, 205101 (2011).
- [7] Z. Wang, H. Weng, Q. Wu, X. Dai, and Z. Fang, *Phys. Rev. B* **88**, 125427 (2013).
- [8] Z. K. Liu, J. Jiang, B. Zhou, Z.J. Wang, Y. Zhang, H. M. Weng, D. Prabhakaran, S.-K. Mo, P. D. H. Peng an, T. Kim *et al.*, *Nat. Mater.* **13**, 677 (2014).
- [9] S. Borisenko, Q. Gibson, D. Evtushinsky, V. Zabolotnyy, B. Büchner, and R. J. Cava, *Phys. Rev. Lett.* **113**, 027603 (2014).
- [10] M. Neupane, S.-Y. Xu, R. Sankar, N. Alidoust, G. Bian, C. Liu, I. Belopolski, T.-R. Chang, H.-T. Jeng, H. Lin *et al.*, *Nat. Commun.* **5**, 3786 (2014).
- [11] H. Yi, Z. Wang, C. Chen, Y. Shi, Y. Feng, A. Liang, Z. Xie, S. He, J. He, Y. Peng *et al.*, *Sci. Rep.* **4**, 6106 (2014).

- [12] M. Neupane, S.-Y. Xu, N. Alidoust, R. Sankar, I. Belopolski, D. S. Sanchez, G. Bian, C. Liu, T.-R. Chang, H.-T. Jeng *et al.*, *Phys. Rev. B* **91**, 241114 (2015).
- [13] T. Liang, Q. Gibson, M. N. Ali, M. Liu, R. J. Cava, and N. P. Ong, *Nat. Mater.* **14**, 280 (2015).
- [14] Q. Wang, C.-Z. Li, S. Ge, J.-G. Li, W. Lu, J. Lai, X. Liu, J. Ma, D.-P. Yu, Z.-M. Liao *et al.*, *Nano Lett.* **17**, 834 (2017).
- [15] C. Zhu, X. Yuan, F. Xiu, C. Zhang, Y. Xu, R. Zhang, Y. Shi, and F. Wang, *Appl. Phys. Lett.* **111**, 091101 (2017).
- [16] M. N. Ali, Q. Gibson, S. Jeon, B. B. Zhou, A. Yazdani, and R. J. Cava, *Inorg. Chem.* **53**, 4062 (2014).
- [17] S. Jeon, B. B. Zhou, A. Gyenis, B. E. Feldman, I. Kimchi, A. C. Potter, Q. D. Gibson, R. J. Cava, A. Vishwanath, and A. Yazdani, *Nat. Mater.* **13**, 851 (2014).
- [18] A. Akrap, M. Haki, S. Tchoumakov, I. Crassee, J. Kuba, M. O. Goerbig, C. C. Homes, O. Caha, J. Novák, F. Teppe *et al.*, *Phys. Rev. Lett.* **117**, 136401 (2016).
- [19] R. Sankar, M. Neupane, S.-Y. Xu, C. J. Butler, I. Zeljkovic, I. P. Muthuselvam, F.-T. Huang, S.-T. Guo, S. K. Karna, M.-W. Chu *et al.*, *Sci. Rep.* **5**, 12966 (2015).
- [20] G. Steigmann and J. Goodyear, *Acta Crystallogr.* **24**, 1062 (1968).
- [21] N. Marzari, A. A. Mostofi, J. R. Yates, I. Souza, and D. Vanderbilt, *Rev. Mod. Phys.* **84**, 1419 (2012).
- [22] W. Kohn and L. J. Sham, *Phys. Rev.* **140**, A1133 (1965).
- [23] A. A. Mostofi, J. R. Yates, G. Pizzi, Y.-S. Lee, I. Souza, D. Vanderbilt, and N. Marzari, *Comput. Phys. Commun.* **185**, 2309 (2014).
- [24] J. P. Perdew, K. Burke, and M. Ernzerhof, *Phys. Rev. Lett.* **77**, 3865 (1996).
- [25] P. Giannozzi, S. Baroni, N. Bonini, M. Calandra, R. Car, C. Cavazzoni, D. Ceresoli, G. L. Chiarotti, M. Cococcioni, I. Dabo *et al.*, *J. Phys.: Condens. Matter* **21**, 395502 (2009).
- [26] M. P. López Sancho, J. M. López Sancho, and J. Rubio, *J. Phys. F* **15**, 851 (1985).
- [27] L. Petaccia, P. Vilmercati, S. Gorovikov, M. Barnaba, A. Bianco, D. Cocco, C. Masciovecchio, and A. Goldoni, *Nucl. Instrum. Methods Phys. Res., Sect. A* **606**, 780 (2009).